

Development of sol-gel derived gahnite anti-reflection coating for augmenting the power conversion efficiency of polycrystalline silicon solar cells

GOBINATH VELU KALIYANNAN¹, SENTHIL VELMURUGAN PALANISAMY¹, MANIVASAKAN PALANISAMY², MOHANKUMAR SUBRAMANIAN³, PRABHAKARAN PARAMASIVAM¹, RAJASEKAR RATHANASAMY^{1,*}

¹Kongu Engineering College, Perundurai, Tamil Nadu, 638060, India

²Bharathiar University Arts and Science College, Modakurichi, Tamil Nadu, 638104, India

³Kongunadu College of Engineering and Technology, Trichy, Tamil Nadu, 621215, India

The present research is focused on developing $ZnAl_2O_4$ (gahnite) spinel as an antireflection coating material for enhanced energy conversion of polycrystalline silicon solar cells (PSSC). $ZnAl_2O_4$ has been synthesized using dual precursors, namely aluminum nitrate nonahydrate and zinc nitrate hexahydrate in ethanol media. Diethanolamine has been used as a sol stabilizer in sol-gel process for $ZnAl_2O_4$ nanosheet fabrication. $ZnAl_2O_4$ nanosheet was deposited layer-by-layer (LBL) on PSSC by spin coating method. The effect of $ZnAl_2O_4$ coating on the physical, electrical, optical properties and temperature distribution in PSSC was investigated. The synthesized antireflection coating (ARC) material bears gahnite ($ZnAl_2O_4$) spinel crystal structure composed of two dimensional (2D) nanosheets. An increase in layer thickness proves the LBL deposition of ARC on the PSSC substrate. The $ZnAl_2O_4$ 2D nanosheet comprising ARC on the PSSC was tested and it exhibited a maximum of 93 % transmittance, short-circuit photocurrent of 42.364 mA/cm² and maximum power conversion efficiency (PCE) 23.42 % at a low cell temperature (50.2 °C) for three-layer ARC, while the reference cell exhibited 33.518 mA/cm², 15.74 % and 59.1 °C, respectively. Based on the results, $ZnAl_2O_4$ 2D nanosheets have been proven as an appropriate ARC material for increasing the PCE of PSSC.

Keywords: *polycrystalline silicon solar cell; sol-gel; spin coating; anti-reflection coatings; gahnite; power conversion efficiency*

1. Introduction

Nowadays, depletion of fossil fuels, which is connected with the production of global energy, is observed. To overcome the intrinsic problem like limited availability and environmental issues related to the use of fossil fuels, new and more sustainable long-term energy solutions are employed to meet the future energy supply. In this regard, for the production of large-scale electricity, one of the alternatives is photovoltaics which converts sunlight directly into electricity. By minimizing the reflection losses, the PCE of solar can be improved by various techniques developed by researchers [1, 2]. In solar cells, display panels, and optical lenses,

antireflection coatings (ARCs) are widely used, which is one of the effective approaches employed to control reflection loss [3]. For example, MgF_2 , Al_2O_3 , Si_xN_x , SiO_x , TiO_2 , Ta_2O_5 , and ZnS are the materials used as ARCs in PSSC [4]. In recent years, owing to their potential optical and electrical properties, metal oxide semiconductors have been widely employed as ARC material.

ZnO is applied for a variety of important potential applications, such as optical and magnetic memory devices, chemical and gas sensors, solar cells, UV-light emitting diodes, piezoelectric transducers, photodetectors, photodiodes, biomedical engineering devices, and others [5]. Silicon solar cells with deposited zinc oxide based ARC thin films are used as transparent conductive thin

*E-mail: rajasekar.cr@gmail.com

film electrodes as they possess appropriate electrical conductivity, optical transparency, non-toxicity, and good stability to plasma environment and can be fabricated at low production cost [6, 7]. Increased consumption of tin-doped indium oxide (ITO) based transparent conductive oxide (TCO) has led to increased cost, low electrical conductivity of $\sim 10^{-4}(\Omega \cdot \text{cm})^{-1}$, toxicity and instability in hydrogen plasma which gave a great motivation for the development of alternative transparent conducting materials. Improving the electrical conductivity and optical transparency of these metal oxides is the main challenge to be overcome. Optical, electrical and magnetic properties of TCO can be improved by alloying with appropriate elements of metal oxides in spinel structures. Consequently, extrinsic dopants such as Ga, In, Al, Cd, Cu, etc. are considered as donors which may alter the band gap of semiconductors. Obviously, Al doping in ZnO lattice induces defects and alters the band gap which may improve the optical and electrical properties of ZnO [5]. ZnO is a n-type wide band gap (3.37 eV) semiconductor that possesses large exciton binding energy (~ 60 meV) [8, 9].

Al-doped ZnO (AZO) films have received considerable attention as transparent conducting electrodes due to their high electrical conductivity, good optical transmittance and simple processing methods [6, 8, 10, 11]. The formation of spinel structured ZnAl_2O_4 (gahnite) is possible due to high concentration of Al dopant in ZnO [12, 13].

In both visible and ultraviolet spectra, ZnAl_2O_4 spinel acts as a transparent conductive oxide film which possesses relatively high energy band gap (3.8 eV), mechanical resistance, thermal properties, fluorescence efficiency, and chemical stability better than other ZnO doped films. For photoelectronic devices and optical coating applications, these improved properties of spinel ZnAl_2O_4 are very desirable [14–16]. For the deposition of ARCs on the surface of photovoltaic cells, former researchers have reported different coating methods such as spin coating, dip coating and spray pyrolysis [6, 8, 17–21]. Only a few studies have been performed to measure and calibrate the temperature field using IR (infrared) thermography by adopting ZnAl_2O_4 ARC coating material.

Therefore, the current research work focuses on employing ZnAl_2O_4 2D nanosheets as an ARC material for enhancing the PCE of polycrystalline silicon solar cells. 2D gahnite (ZnAl_2O_4) nanosheets consisting of spinel nanocrystals have been prepared by using sol-gel technique. The structural, optical, electrical and thermal properties of ZnAl_2O_4 2D nanosheet deposited PSSC were investigated.

2. Experimental

2.1. Materials

Precursors – aluminum nitrate nonahydrate ($\text{Al}(\text{NO}_3)_3 \cdot 9\text{H}_2\text{O}$) and zinc nitrate hexahydrate ($\text{Zn}(\text{NO}_3)_2 \cdot 6\text{H}_2\text{O}$) with 98.5 % purity – were procured from Loba Chemie Private Ltd., India. Ethanol ($\text{C}_2\text{H}_5\text{OH}$) with 99.9 % purity was bought from Changshu Hongsheng Fine Chemicals, China. Stabilizer diethanolamine (DEA) ($\text{NH}(\text{CH}_2\text{CH}_2\text{OH})_2$) with 98.5 % purity was procured from Merck Life Science Private Ltd., India. PSSC (52 mm \times 38 mm) was purchased from Eco-Worthy, China.

2.2. Methodology

Fig. 1 depicts the pictorial representation of layer by layer synthesis of ZnAl_2O_4 2D nanosheets.

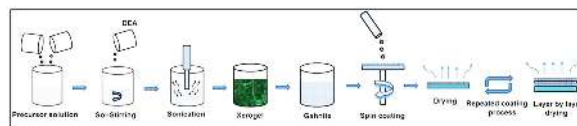


Fig. 1. Pictographic representation of synthesis of LBL assembly.

2.2.1. Preparation of ZnAl_2O_4 2D nanosheets

The ZnAl_2O_4 2D nanosheet was synthesized by dissolving 4.3 g of $\text{Al}(\text{NO}_3)_3 \cdot 9\text{H}_2\text{O}$ and 3.8 g of $\text{Zn}(\text{NO}_3)_2 \cdot 6\text{H}_2\text{O}$ in 100 mL of $\text{C}_2\text{H}_5\text{OH}$. The precursor solution was stirred for 45 min. Further, 20 mL $\text{NH}(\text{CH}_2\text{CH}_2\text{OH})_2$ was added as a forming agent for stabilization. The solution was sonicated for 10 minutes followed

by continuous stirring for 2 h to obtain a pure homogeneous solution. The solution was then kept in a hot air oven at 150 °C for 15 h. During the vaporization process, the pale white color solution turned into black jelly paste. Finally, ZnAl₂O₄ 2D nanosheets were obtained from xerogel (black jelly paste) after calcination operation held at 550 °C for 2 h.

2.2.2. LBL assembly

The coating solution was prepared by dissolving the obtained ZnAl₂O₄ 2D nanosheets (1 g) in 100 mL of C₂H₅OH followed by continuous stirring for 2 h using a magnetic stirrer at room temperature. Before coating, the PSSC surface was washed with C₂H₅OH. The ZnAl₂O₄ 2D nanosheet dispersion was deposited on PSSC substrate by spin coating technique [22]. A solution containing ZnAl₂O₄ was dropped on the substrate. The parameters adopted for coating and drying are shown in Table 1.

The disc was constantly rotated at a speed of 3000 rpm for 30 seconds followed by drying in the hot air oven at 100 °C for 10 minutes. The coating and drying processes were repeated for formation of LBL assembly. From the FE-SEM image, the thickness of deposited layers (1-5) was measured and shown in Table 1. The gradual increase in the thickness (Table 1) confirms the uniformity of LBL deposition on the substrate.

2.3. Characterization methods

The crystal phase and crystalline orientation of the ZnAl₂O₄ 2D nanosheets were determined by X-ray diffraction (XRD), using Model X'PertPro analyzer, PANalytical, Netherlands, operated at 40 kV and 30 mA with CuK α radiation wavelength of 1.525 Å and scanning rate of 0.5° per minute at a step size of 0.02°. The energy dispersive X-ray fluorescence spectrometer (XRF, Model EDX-720, Shimadzu, Japan) was used to analyze the chemical composition of the sample calcined at 550 °C. Thermal analysis of the xerogel was performed using thermogravimetric/differential thermal analyzer (TG/DTA, Model SII 6300, EXSTAR, USA) in order to study the evaporation, decomposition and crystallization temperatures.

High-resolution transmission electron microscope (HR-TEM, Model: JEM 2100, Jeol, Japan) was employed to analyze the surface morphology and microstructure of the ZnAl₂O₄ sample. Further, the transmittance was recorded by ultraviolet visible spectroscopy (UV-Vis-NIR, Model Varian-Cary 5000, USA). The coating thickness and surface morphology of the ZnAl₂O₄ 2D nanosheets were examined by field emission scanning electron microscope (FE-SEM, Model MIRA 3, TESCAN, USA). I-V characteristics of ZnAl₂O₄ 2D nanosheet coated and uncoated silicon solar cells were measured using Keithley 2450 source meter (Tektronix, USA). Temperature studies of the coated and uncoated silicon solar cells were performed by infrared thermal imaging (IR Thermal imager, Model Ti100 Series, Fluke, USA) technique.

3. Results and discussion

Fig. 2 depicts an XRD pattern of powder ZnAl₂O₄ 2D nanosheets calcined at 550 °C. The obtained Miller indices values (2 2 0), (3 1 1), (4 0 0), (4 2 2), (5 1 1), (4 4 0) and position of interference peaks of the synthesized ZnAl₂O₄ 2D nanosheets are in accordance with the standard interference peaks (JCPDS Card No. 1-1146) as shown in Fig. 2.

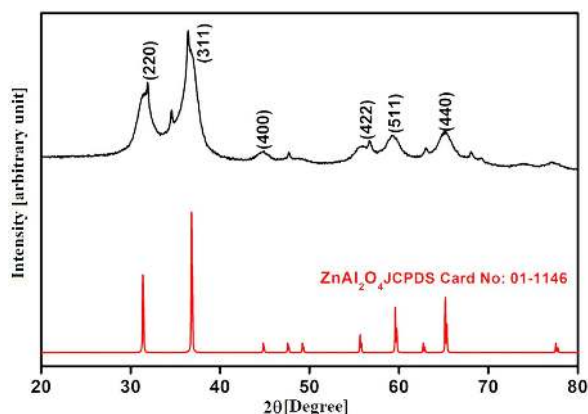
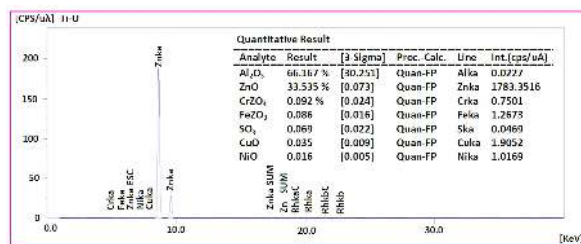


Fig. 2. XRD pattern of ZnAl₂O₄ 2D nanosheets.

Fig. 3 shows the XRF plot and the corresponding elemental percentage composition for synthesized material. From the quantitative results,

Table 1. Deposition parameters for LBL assembly.

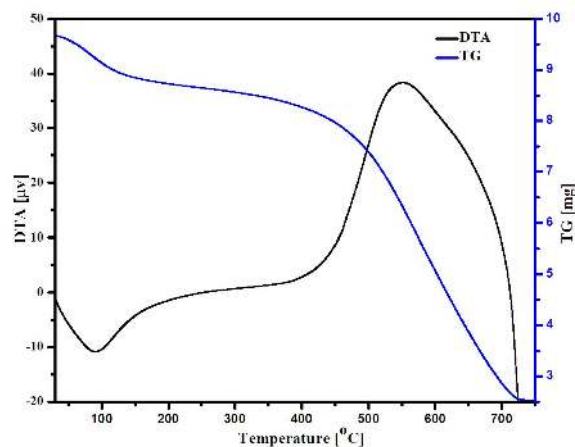
Number of layers	Spin coating speed [rpm]	Time duration [s]	Layer thickness [μm]	Drying temperature [$^{\circ}\text{C}$]
Layer 1			0.55	
Layer 2	3000	30	1.05	100
Layer 3			1.56	
Layer 4			2.15	
Layer 5			2.56	

Fig. 3. XRF chemical composition of ZnAl₂O₄ 2D nanosheets.

it is proven that AlO₃ is the major component followed by ZnO in the formation of ZnAl₂O₄ spinel crystal structure.

Fig. 4 shows the TG/DTA curves of the xerogel. The TG plot shows the first weight loss at 100 °C which is due to the evaporation of C₂H₅OH and interlayer water [23, 24]. The endothermic peak in the range of 250 °C to 450 °C corresponds to the second weight loss due to the combustion of organic matters, like NH(CH₂CH₂OH)₂ and alcohol groups. The final weight loss temperature at 540 °C (exothermic peak) is attributed to the combustion of ZnAl₂O₄ spinel structure. From Fig. 4, it can be seen that the thermal decomposition of the xerogel takes place before 550 °C and ZnAl₂O₄ spinel crystal structure is formed at 550 °C.

The characteristic TEM and HR-TEM images with selected area electron diffraction (SAED) pattern of ZnAl₂O₄ 2D nanostructures are shown in Fig. 5. TEM images reveal that the obtained ZnAl₂O₄ spinel crystal structure has 2D morphology with the formation of nanosheets composed of nanoparticles. Fig. 5 presents 2D structure of the nanosheets which are composed of particles with the size of 8 nm to 16 nm. Based on the HR-TEM

Fig. 4. TG/DTA plot of ZnAl₂O₄ xerogel.

images shown in Fig. 5, the length and the width of the nanosheets are in the range of 2 μm to 4 μm and 1 μm to 2 μm , respectively, indicating that the nanosheets have the aspect ratio of 2:1. The lattice fringe spacing of 0.28 nm, shown in Fig. 5c is in agreement with the d-spacing between the (2 2 0) crystallographic planes of ZnAl₂O₄ cubic spinel system, which is confirmed by the XRD pattern. The dotted ring pattern of SAED in Fig. 5d shows the polycrystalline structure of the ZnAl₂O₄ nanosheet cubic crystal system.

The 1 wt.% of ZnAl₂O₄ nanosheets were coated by layer 1, layer 2, layer 3, layer 4 and layer 5 on the top of PSSC. Fig. 6a to Fig. 6c show the cross sectional FE-SEM images of layer 2 (Fig. 6a), layer 3 (Fig. 6b), layer 4 (Fig. 6c) coating of ZnAl₂O₄. The images prove the deposition of the layers on the PSSC substrate. The thicknesses of the deposited layers, namely layer 2, layer 3, layer 4 are 1.05 μm ,

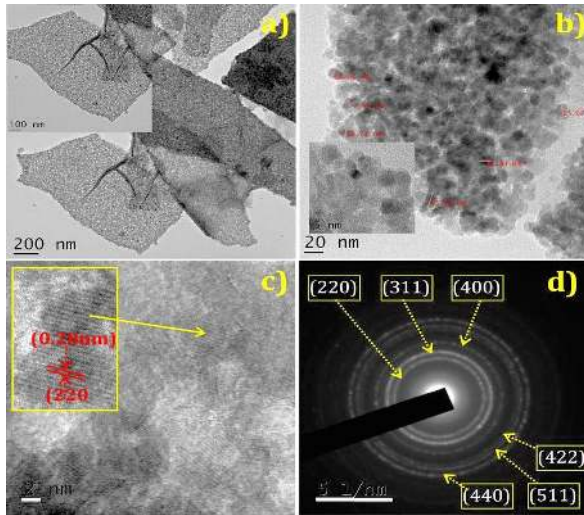


Fig. 5. TEM images (a and b), HR-TEM image (c) and SAED pattern (d) of ZnAl_2O_4 2D nanosheets.

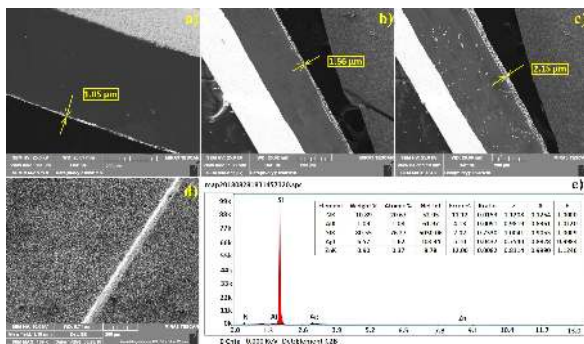


Fig. 6. Cross sectional FE-SEM images of ARC coated (a) layer 2, (b) layer 3, (c) layer 4, (d) FE-SEM image of ZnAl_2O_4 nanosheet coated silicon solar cell and (e) EDS of thin films of ZnAl_2O_4 nanosheets on silicon solar cells.

1.56 μm and 2.15 μm , respectively. Fig. 6d shows the surface morphology of layer 3 deposited on PSSC and the corresponding Energy Dispersive Spectrum (EDS) analysis is shown in Fig. 6e. Si is the major component of the PSSC substrate. In addition, small amounts of Al and Zn are evident, proving the formation of ZnAl_2O_4 layer on the PSSC. The traces of Al and Zn from the deposited layer can be correlated with XRF results of pure ZnAl_2O_4 2D nanosheets.

Fig. 7 shows the optical transmittance of the ZnAl_2O_4 nanosheet layers deposited by spin

coating on a glass slide surface. ZnAl_2O_4 coated PSSC substrates exhibit the best transmittance in the wavelength range of 300 nm to 800 nm. It can be clearly seen from Fig. 7 that the three layer coating of ZnAl_2O_4 nanosheets exhibits superior transmittance of 93 %, since ZnAl_2O_4 scatters photons of irradiated light in maximum amounts so as more photons can pass through the glass slide substrate [25–29]. It can be clearly seen from Fig. 6 that the deposition of ZnAl_2O_4 nanosheets enhances the transmittance of irradiated light with minimal reflection compared to uncoated PSSC substrate. The ZnAl_2O_4 nanosheet has the optical band gap value of 3.8 eV which confirms that the material is a transparent semiconductor [14]. Further, the quality of improved transmittance of ZnAl_2O_4 nanosheet makes an efficient surface layer for enhanced light trapping in the photovoltaic cell. The optical transmittance gradually rises from one layer to three layer coating, while the transmittance of the coating with four and five layers decreases. This evidences the importance of optimization of ZnAl_2O_4 nanosheet layers thickness in ARCs and shows the significance of layer thickness, and coating transparency for the efficiency of photovoltaic cells. Moreover, the transmittance loss in layer 4 and layer 5 is due to the aggregation of ZnAl_2O_4 nanosheets in the layers causing increased light scattering.

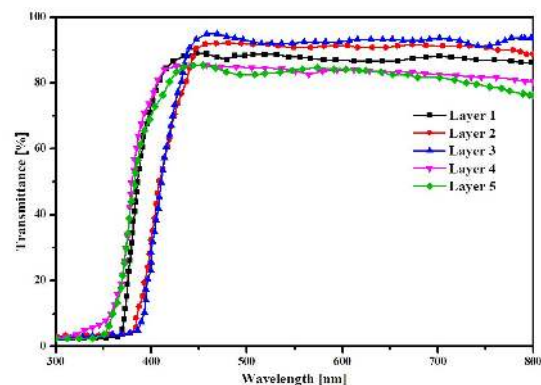


Fig. 7. Optical transmittance of thin films of ZnAl_2O_4 nanosheets.

To evaluate the enhanced power conversion efficiency of ZnAl_2O_4 nanosheets modified PSSC, I-V characteristics were measured in controlled

atmospheric conditions. Fig. 8 displays the experimental setup for I-V characterization. The fabricated solar simulator containing neodymium daylight lamp (radiation) was adjusted to the required radiation level with the help of AC regulator. The controlled atmospheric conditions nullified the continuous periodic fluctuations of radiation that normally occur in open atmospheric condition. A pyrometer was used to measure the radiation of neodymium lamp. IR thermal imaging was employed to assess the temperature distribution in both pure and AR coated silicon solar cells.

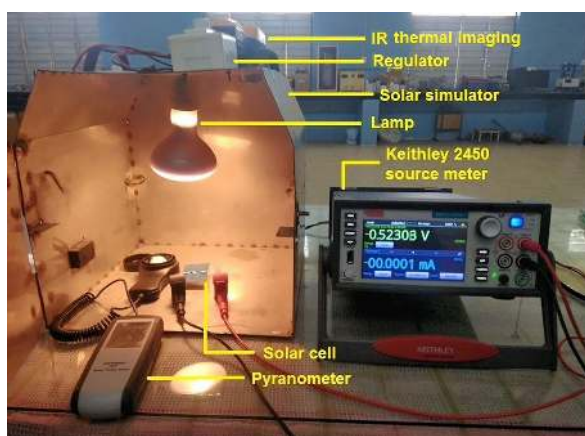


Fig. 8. Setup for I-V measurement under controlled atmospheric conditions.

Fig. 9 shows photovoltaic characteristics (I-V curves) of ZnAl_2O_4 nanosheet coated and uncoated PSSCs illuminated by neodymium lamp radiation of 100 mW/cm^2 under controlled atmospheric conditions.

The efficiency of uncoated (bare) and coated PSSCs was determined from I-V curves and has been summarized in Table 2. The uncoated PSSC produced the PCE of 15.74 % ($I_{sc} = 33.518 \text{ mA/cm}^2$, $V_{oc} = 0.632 \text{ V}$, $FF = 0.75$). 3 layer coating of 1 wt.% ZnAl_2O_4 nanosheet on the silicon solar cell gave superior short-circuit photocurrent ($I_{sc} = 42.364 \text{ mA/cm}^2$), open circuit-voltage ($V_{oc} = 0.70 \text{ V}$) and fill factor ($FF = 79 \%$). Accordingly, high I_{sc} and V_{oc} resulted in raising the PCE from 15.74 % to 23.42 %. Particularly, ZnAl_2O_4 thin film consisting of 3 layers showed the highest PCE in comparison with uncoated cell.

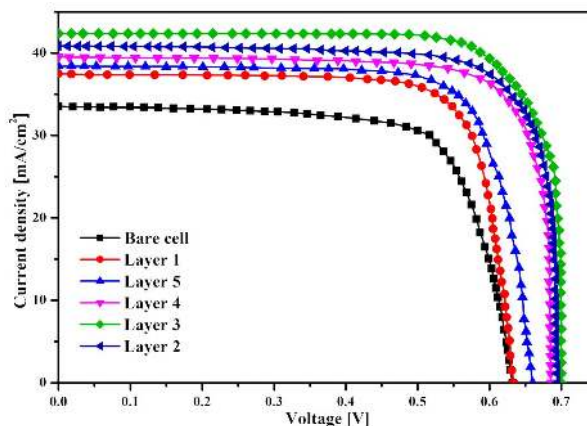


Fig. 9. Photovoltaic characteristics of bare and ZnAl_2O_4 coated PSSC under controlled atmospheric conditions.

Further, the higher number of layers deposited on PSSC led to drop in I_{sc} and V_{oc} with the consecutive decrease in PCE.

The uncoated and coated PSSCs were subjected to temperature measurement under controlled atmospheric conditions. The efficiency η of the photovoltaic cell decreased with the rise in cell temperature [30, 31]. IR temperature measurement employs a non-contact method for studying the temperature changes in various fields such as medical, aeronautical and manufacturing industries. This technique produces visual pictures of the temperature of silicon solar cells conveying information faster and easier [32]. Fig. 10 shows the experimental results of temperature measurement on uncoated cell (Fig. 10a), and cells coated with layer 1 (Fig. 10b), layer 2 (Fig. 10c), layer 3 (Fig. 10d), layer 4 (Fig. 10e) and layer 5 (Fig. 10f). It can be clearly seen that the layer 3 coated cell shows lower cell temperature ($50.2 \text{ }^\circ\text{C}$) when compared with other PSSCs. Increased light scattering raises the heat flux in the layer, but decreases the transparency which is confirmed by IR thermal imaging of ARCs. Therefore, it is evident that the low cell temperature significantly increases the PCE of PSSC.

The generated cell temperature was minimal for ZnAl_2O_4 nanosheet coated PSSC, which indeed enhanced the PCE of the cell. This may be due to the (i) increase in charge carrier mobility, (ii) lower

Table 2. Photovoltaic characteristics of thin films of ZnAl₂O₄ nanosheet coated PSSC compared with uncoated PSSC.

PSSC	I _{sc} [mA/cm ²]	V _{oc} [V]	Fill factor [%]	Efficiency η [%]
Bare cell	33.518	0.632	75	15.88
Layer 1	37.487	0.634	76	18.06
Layer 2	40.869	0.692	76	21.49
Layer 3	42.364	0.700	79	23.42
Layer 4	39.541	0.686	76	20.61
Layer 5	38.411	0.667	76	19.47

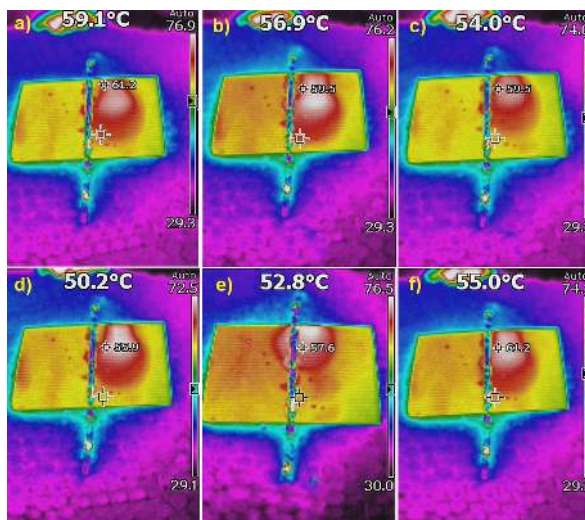


Fig. 10. Temperature measurement of bare and coated silicon solar cells.

phonon-electron scattering and (iii) increased p-n junction built-in voltage of PSSC.

4. Conclusions

A facile sol-gel route was employed to synthesize ZnAl₂O₄ nanosheets using dual precursors: zinc nitrate hexahydrate and aluminum nitrate nonahydrate with ethanol as a solvent and diethanolamine as a stabilizer. The Miller indices (2 2 0), (3 1 1), (4 0 0), (4 2 2), (5 1 1) and (4 4 0) obtained from XRD results were indexed to ZnAl₂O₄ spinel crystal structure. The percentage of Al₂O₃ (66 %) and ZnO (33 %) obtained from XRF quantitative results confirmed the formation of ZnAl₂O₄ spinel. From HR-TEM study, it was evident that the ZnAl₂O₄ 2D nanosheets are

made from ZnAl₂O₄ particles with a size of 8 nm to 16 nm. The increase in layer thickness confirmed the deposition of layers on the polycrystalline silicon solar cell substrate. The superior transmittance of 93 % and PCE of 42.36 % have been obtained for three-layer ZnAl₂O₄ deposited PSSC evidencing diffusion of more photons into the silicon solar cell substrate. Based on the observations from I-V studies, the PSSC with deposited three-layer ZnAl₂O₄ showed the highest I_{sc} of 42.364 mA/cm², which significantly enhanced the PCE to 23.42 %. Further increase in the number of deposited layers led to decrease in PCE. It was also observed that the efficiency of silicon solar cell drops with the rise in solar cell temperature. Hence, it is obvious that ZnAl₂O₄ nanosheet acted as an excellent ARC material for increasing the PCE of PSSC.

Acknowledgements

This research is supported by the Science and Engineering Research Board (SERB), Department of Science and Technology (DST), Government of India, under the Start-Up Research Grant for Young Scientist (Project Grant No.: YSS/2015/001151).

References

- [1] KATHIRVEL K., RAJASEKAR R., SHANMUHARAN T., PAL S.K., SATHISH KUMAR P., SARAVANA KUMAR J., *Mater. Sci.-Poland.*, 35 (2017), 181.
- [2] KEMELL M., RITALA M., LESKELA M., *Crit. Rev. Solid. State.*, 30 (2005), 1.
- [3] LIEN S.Y., WUU D.S., YEH W.C., LIU J.C., *Sol. Energ. Mat. Sol. C.*, 90 (2006), 2710.
- [4] SHARMA R., AMIT G., AJIT V., *J. Nano- Electron. Phys.*, 9(2017), 1.
- [5] AL-GHAMDI A.A., AL-HARTOMY O.A., OKR M.E., NAWAR A.M., GAZZAR S.E., TANTAWY F.E., YAKUPHANOGLU F., *Spectrochim. Acta A*, 131 (2014), 512.

- [6] VERMA A., KHAN F., KUMAR D., KAR M., CHAKRAVARTY B.C., SINGH S.N., HUSAIN M., *Thin Solid Films*, 518 (2010), 2649.
- [7] BALAPRAKASH V., GOWRISANKAR P., SUDHA S., RAJKUMAR R., *Mater Technol.*, 33 (2018), 420.
- [8] SHAHID M.U., DEEN K.M., AHMAD A., AKRAM M.A., ASLAM M., AKHTAR W., *Appl. Nanosci.*, 6 (2016), 235.
- [9] BAHADUR H., SRIVASTAVA A.K., SHARMA R.K., CHANDRA S., *Nanoscale Res. Lett.*, 2 (2007), 469.
- [10] ROZATI S.M., AKESTEH S.H., *Mater. Charact.*, 58 (2007), 319.
- [11] YOO J., LEE J., KIM S., YOON K., PARK I.J., DHUNGEL S.K., KARUNAGARAN B., MANGALARAJ D., YI J., *Thin Solid Films*, 480 (2005), 213.
- [12] WIFF J.P., KINEMUCHI Y., KAGA H., ITO C., WATARI K., *J. Eur. Ceram. Soc.*, 29 (2009), 1418.
- [13] DIXIT H., TANDON N., COTTENIER S., SANIZ R., LAMOEN D., PARTOENS B., *Phys. Rev. B*, 87 (2013), 174101.
- [14] CIUPINA V., CARAZEANU I., PRODAN G., *J. Optoelectron. Adv. M.*, 6 (2004), 1317.
- [15] WANG S.F., SUN G.Z., FANG L.M., LEI L., XIANG X., ZU X.T., *Sci. Rep.*, 5 (2015) 12849.
- [16] ZOU L., LI F., XIANG X., EVANS D.G., DUAN X., *Chem. Mater.*, 18 (2006), 5852.
- [17] MUSAT V., TEIXEIRA B., FORTUNATO E., MONTEIRO R.C.C., VILARINHO P., *Surf. Coat. Tech.*, 180 (2004), 659.
- [18] VERMA A., VIJAYAN N., *J. Mater. Res.*, 28 (2013), 2990.
- [19] BOUKHENOUBA N., MAHAMDI R., RECHEM D., *J. Semicond.*, 37 (2016), 113001.
- [20] RAVICHANDRAN K., JABENA BEGUM N., SNEGA S., SAKTHIVEL B., *Mater. Manuf. Process.*, 31 (2016), 1411.
- [21] CHEN D., *Sol. Energ. Mat. Sol. C.*, 68 (2001), 313.
- [22] NATSUME Y., SAKATA H., *Thin solid films*, 372 (2000), 30.
- [23] SILVA A.A.D., SOUZA GONCALVES A.D., DAVOLOS M.R., *J. Sol-Gel Sci. Techn.*, 49 (2009), 101.
- [24] WEI X., CHEN D., *Mater. Lett.*, 60 (2006), 823.
- [25] AMIN P.O., KADHIM A.J., AMEEN M.A., ABDULWAHID R.T., *J. Mater. Sci-Mater. El.*, 29 (2018), 16010.
- [26] HABUBI N.F., ISMAIL R.A., MISHJIL K.A., HASSOON K.I., *Silicon*, (2018), 1-6.
- [27] TAHERNIYA A., RAOUFI D., *Mater. Res. Express.*, 6 (2018), 016417.
- [28] KESMEZ O., AKARSU E., CAMURLU H.E., YAVUZ E., AKARSU M., ARPAC E., *Ceram. Int.*, 44 (2018), 3183-3188.
- [29] JUNG J., JANNAT A., AKHTAR M.S., YANG O., *J. Nanosci. Nanotechnol.*, 18 (2018), 1274-1278.
- [30] RADZIEMSKA E., *Renew. Energ.*, 28 (2003), 1.
- [31] DUBEY S., SARVAIYA J.N., SESHADRI B., *Energy Procedia*, 33 (2013), 311.
- [32] KUMAR J., NEGI V.S., CHATTOPADHYAY K.D., SAREPAKA R.V., SINHA R.K., *Measurement*, 102 (2017) 96.

Received 2018-10-15
Accepted 2019-04-23